Editor's Choice

Recognizable phenotypes associated with intracranial calcification

JOHN H LIVINGSTON[1] | STAVROS STIVAROS[2] | MARJO S VAN DER KNAAP[3] | YANICK J CROW[4]

1 Department of Paediatric Neurology, Leeds General Infirmary, Leeds **2** Imaging, Genomics and Proteomics Research Group, University of Manchester, Manchester, UK **3** Department of Child Neurology, VU University Medical Center, Amsterdam, Netherlands **4** Department of Genetic Medicine, University of Manchester, Manchester Academic Health Science Centre, Central Manchester Foundation Trust University Hospitals, Manchester, UK.

Correspondence to Dr John H Livingston at Department of Paediatric Neurology, F Floor, Martin Wing, Leeds General Infirmary, Leeds LS1 3EX, UK. E-mail: jh.livingston@leedsth.nhs.uk

This article is commented on by Poretti et al. on pages 7–8 of this issue.

PUBLICATION DATA
Accepted for publication 16th July 2012.
Published online 1st November 2012.

ABBREVIATIONS

AGS	Aicardi–Goutières syndrome
BLC–PMG	Band-like calcification with simplified gyration and polymicrogyria
CMV	Cytomegalovirus
CRMCC	Cerebroretinal microangiopathy with calcifications and cysts
ICC	Intracranial calcification
LCC	Leukoencephalopathy with calcification and cysts

AIM In this observational study, we adopted a systematic approach to the radiological phenotyping of disorders associated with intracranial calcification, with the aim of determining if characteristic patterns could be defined as an aid to the future diagnosis of known conditions and the identification of new disorders.
METHOD A cranial imaging-based scoring system was devised using both computed tomography and magnetic resonance imaging data. Patients were grouped into diagnostic categories where a definitive molecular diagnosis was known, or where the clinical and radiological features suggested a specific diagnosis. For patients in whom the diagnosis was unknown, subgroups were defined according to shared radiological features.
RESULTS Data on 244 scans from 119 patients were analysed. A specific diagnosis was available for 59 patients (31males, 28 females; median age 50mo, range 1wk to 54y). These were as follows (number of patients in brackets): Aicardi–Goutières syndrome (33), cerebroretinal microangiopathy with calcification and cysts (10), band-like calcification with simplified gyration and polymicrogyria (6), *COL4A1*-related disease (3), Degos disease (2), Krabbe disease (2), Alexander disease (1), mitochondrial disease (1), and tetrasomy 15 (1). In 60 patients the aetiology was unknown. Within this group, subsets demonstrating shared characteristics suggestive of a specific calcification phenotype could be identified.
INTERPRETATION This study confirms the value of a systematic approach to radiological phenotyping of disorders associated with intracranial calcification.

Intracranial calcification (ICC) occurs in many different neurological disorders, both acquired and genetic, and may be seen in asymptomatic individuals. As such, the presence of ICC is likely to reflect a diversity of pathologies.

From a clinical perspective, the identification of ICC represents a common diagnostic starting point for the physician and may provide an important clue to the underlying diagnosis. However, perhaps because ICC is thought of as an epiphenomenon of low diagnostic specificity, there has been, to our knowledge, no systematic study of the radiological phenotypes associated with ICC. Those reports that have been published relate only to small case series of specific diseases or lists of diverse disorders associated with ICC.

The value of a systematic approach to defining radiological phenotypes has been convincingly demonstrated for the leukoencephalopathies,[1–3] and for disorders of neuronal migration and other brain malformations.[4–6] Such a strategy has enabled the characterization and earlier diagnosis of specific disorders, and the identification of previously unrecognized diseases. In turn, radiological phenotyping has facilitated the identification of causative genes. Here, we present data to illustrate that adopting a systematic approach to the radiological phenotyping of ICC, taken in clinical context, allows the definition of specific disorders associated with that radiological finding. Furthermore, new phenotypes can be identified and the underlying genetic basis, where relevant, determined.

METHOD

Case ascertainment

This is a selected population comprising patients whose clinical details and scans were sent to the authors (YJC, JHL, MSvdK) for a diagnostic opinion. Because of the particular interest of two of the authors (YJC, JHL) in Aicardi–Goutières syndrome (AGS), most patients were referred initially because they were suspected as having a diagnosis of AGS. During the course of this work, it became apparent that there were many patients with ICC in whom a diagnosis of AGS could be excluded with a high degree of confidence on clinical, radio-

 DOI: 10.1111/j.1469-8749.2012.04437.x

logical, and genetic grounds. Thus, there is a bias towards AGS and disorders where, at the time of referral, the diagnosis was unknown. The sample is also biased towards the paediatric age range, although we have not excluded adult patients.

Definitions

ICC was defined as the presence of presumed calcification within the parenchyma of the brain on computed tomography (CT). Calcification was presumed when there were abnormal areas of high density, of a Hounsfield unit value consistent with calcification, within the brain parenchyma.

Data collation

Demographic details and clinical features were documented for all cases. An imaging-based scoring system for radiological phenotypic description was devised, and the results stored on separate CT and magnetic resonance imaging (MRI) databases. The CT database (Table SIa, online supporting information) comprises 31 major categories, and the MRI database (Table SIb online supporting information) 24 categories. All scans were scored by two of the authors (JHL, YJC), and selected scans by a third author (MSvdK). The location and appearance of the calcification was documented and described using a limited number of terms. These were spots, lines, blush, rock, deep gyral, superficial gyral (or gyriform), and reticular. Representative images illustrating these features are shown in Figure 1.

Table I: Summary of patient computed tomography and magnetic resonance imaging characteristics and aetiological groupings

	CT database	MRI database
Number of scans	**140**	**104**
Two	12	18
Three	3	1
Four	1	
Number of patients (male)	119 (59)	84 (48)
Median age (mo) (range)	18 (1wk–59y)	10 (1wk–54y)
Aetiology identified	**49**	**34**
AGS (mutation positive)	33 (27)	23 (19)
BLC	6	5
COL4A1 mutation	3	3
Krabbe disease	2	1
Degos disease	2	1
Juvenile Alexander disease	1	1
Mitochondrial disease	1	1
Chromosomal abnormality (tetrasomy 15)	1	
CRMCC	**10**	**9**
Aetiology unknown	**60**	**41**
Possible destructive mechanism	11	11
With polymicrogyria	6	5
Predominantly grey matter	4	3
Unique familial phenotype	3	
Predominantly white matter	2	2
Familial (dominant) ICC	7	1

CT, computed tomography; MRI, magnetic resonance imaging; AGS, Aicardi–Goutières syndrome; BLC, band-like calcification with simplified gyration and polymicrogyria; CRMCC, cerebroretinal microangiopathy with calcification and cysts; ICC, intracranial calcification.

What this paper adds

- A systematic approach to radiological phenotyping allows recognizable patterns of intracranial calcification to be identified.
- Characteristic patterns of intracranial calcification are seen in a range of disorders.
- Other calcification phenotypes occur, some of which may represent distinct disease entities.
- For optimal diagnostic yield, CT and MRI should be considered together.

Diagnostic categories

Patients were grouped into diagnostic categories where a definitive molecular diagnosis was known, or where the clinical and radiological features suggested a specific diagnosis with a high probability. For patients where the diagnosis was unknown, we defined subgroups according to shared radiological features. In some of these groups the radiological and clinical features were suggestive of a discrete aetiology (see below). However, because these designations are putative at this stage, these patients were classified in the unknown category. The primary diagnostic categories are described below.

Aicardi–Goutieres syndrome

The diagnostic criteria for AGS were a confirmed molecular diagnosis (bi-allelic mutations in *TREX1*, *RNASEH2A*, *RNASEH2B*, *RNASEH2C*, or *SAMHD1*), or, where no molecular confirmation was available, a clinical and laboratory phenotype suggestive of AGS (i.e. an early-onset encephalopathy, negative investigations for common prenatal infections, and a cerebrospinal fluid lymphocytosis of more than five cells per cubic millimetre and/or more than 2 IU/mL of interferon-α). By definition, all patients had ICC.

Band-like calcification with simplified gyration and polymicrogyria (BLC–PMG)

The radiological features of this syndrome are an extensive, bilateral cortical malformation with very simplified gyration and polymicrogyria, particularly in the frontoparietal regions, intracortical band or ribbon-like calcification, and symmetrical thalamic calcification.[7–9] Five of the patients included had bi-allelic mutations in the *OCLN* gene.[10]

Cerebroretinal microangiopathy with calcifications and cysts (CRMCC)

We have included CRMCC as a diagnostic category in view of its striking, and highly characteristic, radiological features.[11,12] At the time of the data analysis, it was not known whether all patients grouped under the umbrella term CRMCC had the same condition, or if one or more genetic disorder could result in the same, or a very similar, radiological phenotype. Specifically, it was unclear whether the disorders previously called Coats plus[13] and leukoencephalopathy with calcification and cysts (LCC)[14] were distinct entities. For this reason we assigned a label of CRMCC to patients whose neuroimaging demonstrated all of the following three features: (1) a leukoencephalopathy (which may be asymmetrical/unilateral); (2) dense calcification of deep nuclei, deep cortex and/or white matter, brainstem and/or

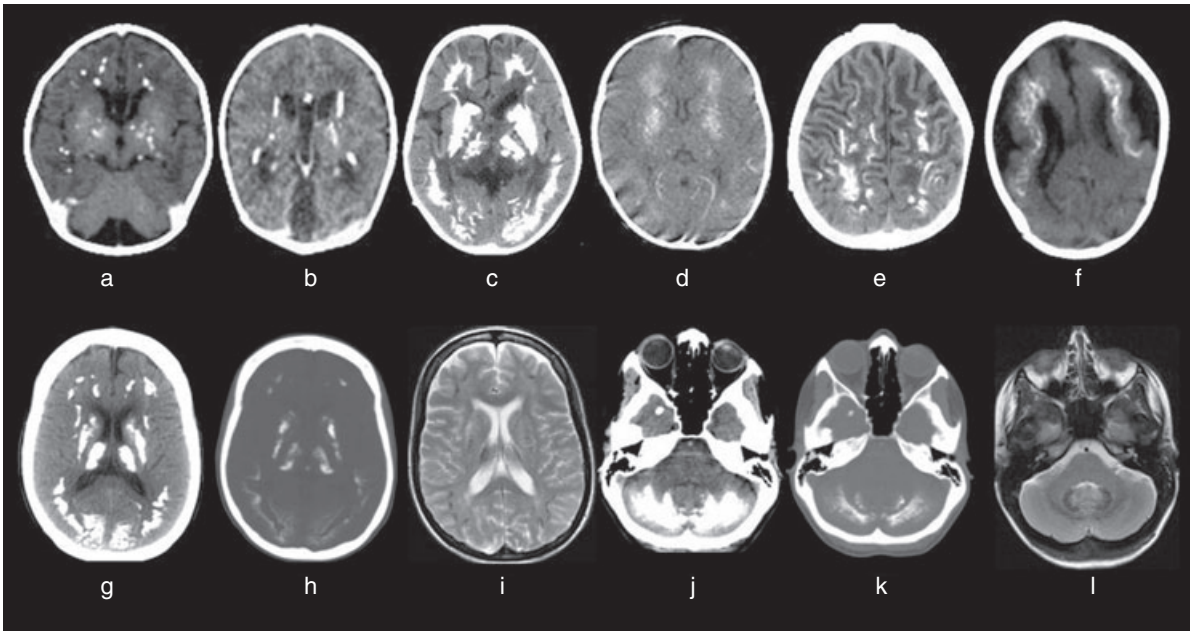

Figure 1: Examples of types of calcification and terminology. (a) spots, (b) lines, (c) rock, (d) blush, (e) gyriform/band-like, (f) reticular. Computed tomography (CT) at normal brain window settings (g, j), CT at bony window setting (h, k), axial T2 magnetic resonance images (i, l), illustrating how different window settings or imaging modalities may be needed to determine the location of calcification. In this example, calcification is exclusively in the grey matter, i.e. basal ganglia, deep cortex, cerebellar folia, and dentate nucleus.

cerebellum; and (3) intraparenchymal cysts. We have recently shown that mutations in *CTC1*, encoding conserved telomere maintenance component 1, cause Coats plus.[15] Mutations were not identified in any patient with an exclusively neurological disorder, indicating that LCC and Coats plus are distinct entities (see Discussion).

Other specific diagnoses

In some patients a specific aetiology for ICC was assigned on the basis of other clinical, laboratory, or radiological findings.

Data analysis

This was an observational study in which images were reviewed by the authors (JHL, YJC, MSvdK), looking for phenotypically recognizable patterns within the imaging data by manual inspection and pattern recognition. This approach allowed subgroups to be identified on the basis of shared radiological features. By definition, CT scans were available for all patients. MRI data were available for most but not all patients, and these data were analysed separately. Clinical features and laboratory results, including molecular testing, were also taken into consideration. Similarly, these data sources were used to characterize further the neuroradiological features of known disorders.

Scans were obtained as part of continuing clinical care, and from patients recruited into an ongoing study of ICC. The study had ethical approval from the Leeds Multi-Centre Research Ethics Committee (reference number 07/Q1206/7).

RESULTS

CT data were available from 119 patients, and MRI data for 84 of these. A summary of all patients is shown in Table I. Most referrals were from the UK and Europe (85), with 20 from North America, 11 from Asia, and three from Australia. Some patients had more than one scan, and the radiological features sometimes evolved with time. The numbers used in the text refer to the number of patients showing a given feature (rather than the number of scans with that feature), and analysis was based on the chronologically earliest scan for a given patient, although where follow-up data were available then temporal evolution in disease appearance was captured.

A specific diagnosis could be assigned in approximately half of all patients, slightly fewer than this if CRMCC is not regarded as a specific diagnosis. For some patients the imaging characteristics suggested the diagnosis and led to confirmatory investigations, including diagnostic molecular testing. This was particularly the case for AGS, BLC–PMG and *COL4A1*-related disease.

Imaging characteristics of patients with a known diagnosis

The details of the calcification patterns and other imaging characteristics are shown in Table SII.

Aicardi–Goutieres syndrome

CT scans were available for 33 patients (42 scans). A classical appearance of calcification can be described (Fig. 2A, a and b). This comprises bilateral spot calcification within the basal ganglia and sometimes thalami, together with spot calcification in the deep white matter of the frontal and parietal lobes.

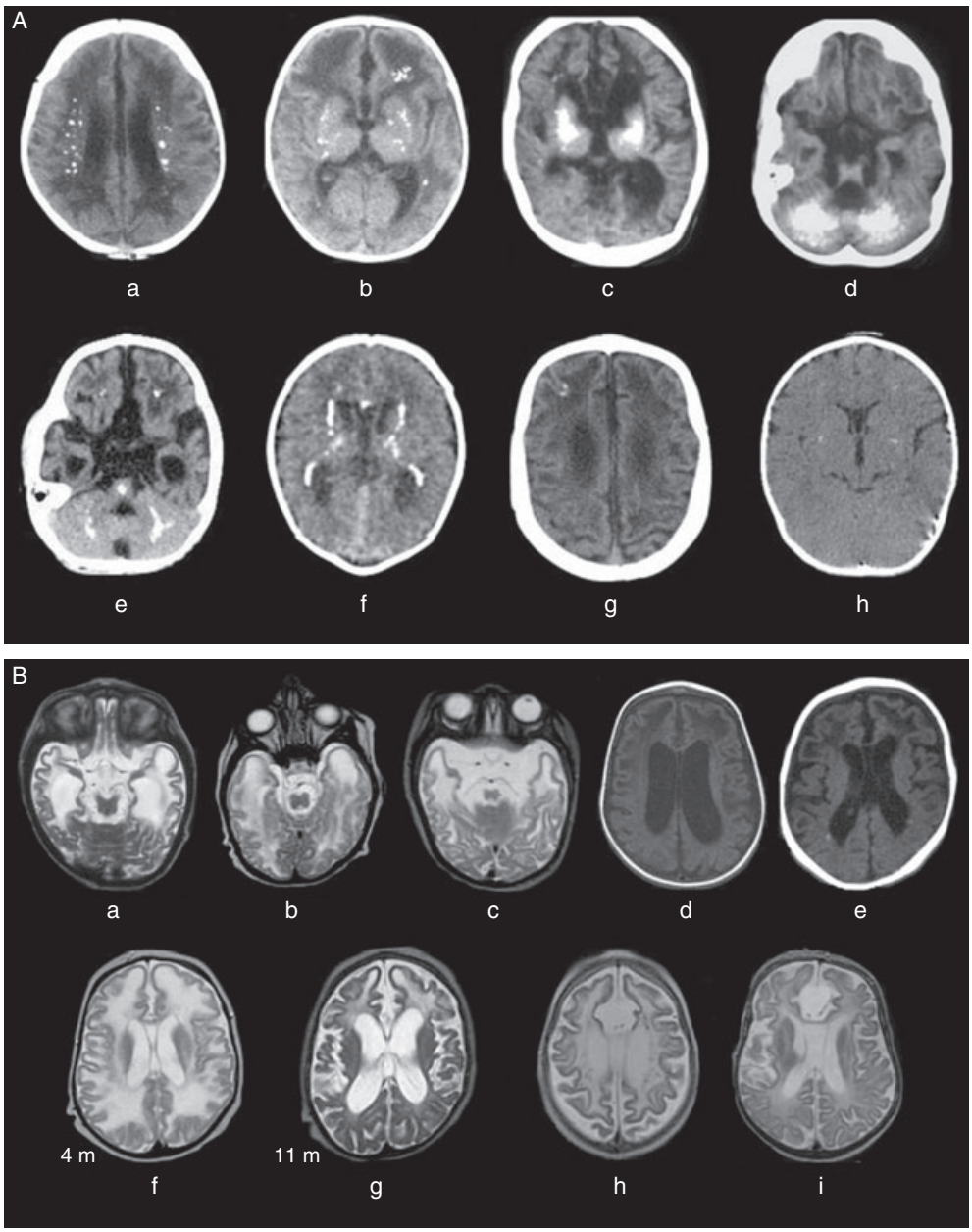

Figure 2: (A) Aicardi–Goutières syndrome computed tomography (CT) appearances. a, b demonstrate the `classical' appearance of spot calcification in the deep cerebral white matter and basal ganglia with low attenuation of the cerebral white matter. Other patterns include rock calcification in the basal ganglia (c), rock calcification in cerebellar white and grey matter (d), pontine calcifications (e), true periventricular, linear calcification (f), subtle cortical calcification in the depth of a sulcus (g), and subtle basal ganglia and white matter calcification (h). (B) Aicardi–Goutières syndrome magnetic resonance (MRI) appearances. Axial T2 images of severe AGS phenotype in three patients (a–c), showing diffuse high signal in the white matter, temporal pole swelling with an apparently simplified gyration of overlying cortex (a, b), and the characteristic pattern of atrophy of the anterior temporal lobe (a, c). The brainstem is hypoplastic. Axial T1 images showing markedly low attenuation of the cerebral white matter with an anterior greater than posterior gradient (d, e). Calcification is apparent (e). Serial axial T2 scans (f, g) showing progression of atrophy, primarily due to loss of white matter volume. T2 axial scans showing the characteristic pattern of frontal lobe atrophy with `pincer-like' appearance due to loss of volume of medial frontal white matter (h, i). Note low signal spots of deep white matter calcification (h).

Calcification in other sites was less common, but could occur in any location. True periventricular (i.e. along the walls of the lateral ventricles) calcification and cortical calcification were uncommon, whereas deep white matter calcification was seen frequently. Progression of calcification was seen in five of seven patients with serial scans. In one patient with four scans, the last one at the age of 10 years, progression arrested after 2.5 years. Typically, the brain and brainstem were atrophic and there was diffuse low density of the cerebral white matter.

MRI scans were available for 23 patients (32 scans) (Fig. 2B). A universal feature was abnormal white matter in the cerebral hemispheres. This was usually diffuse, confluent, and symmetrical, and in all patients involved the periventricular and deep white matter and, in most, the subcortical white matter also. In some of the latter, particularly older patients, the subcortical involvement was patchy with some areas of normal U-fibre myelination. The abnormal white matter often showed an anterior to posterior gradient. In several patients myelination was less than would be expected for chronological age, with many scans showing no normal hemispheric myelination. However, in one patient with mutations in *TREX1*, a follow-up scan at 5 years of age showed that myelination had progressed. Cerebral atrophy was present in most patients, and was clearly progressive in six of nine with serial scans. A characteristic pattern of frontal and/or temporal lobe atrophy was sometimes observed (Fig. 2B, a,c, h and i). Swelling of the anterior temporal lobes and/or the frontal lobes was seen frequently, resulting in an appearance of simplified gyration due to stretching of the cortex (Fig. 2B, a,b). Loss of cerebral white matter volume was a common feature and the brainstem, cerebellum, basal ganglia, and corpus callosum were often atrophic.

Calcification, which was present, by definition, on the CT scans of all patients, was demonstrable on 14 of 32 MRI scans as low signal on T2, high signal on T1, or low signal on gradient-echo sequences. Contrast enhancement occurred in one out of 12 patients to whom it was given.

Band-like calcification with simplified gyration and polymicrogyria (Fig. 3)

CT data were available for six patients, five of whom have biallelic mutations in the *OCLN* gene.[10] Symmetrical cortical calcification was present in all, and usually frontal or frontoparietal. In all patients there was a continuous or semi-continuous ribbon of cortical calcification with, in addition, a reticular pattern in four. All patients had symmetrical thalamic calcification. Pontine calcification was present in four. No patient had cerebellar calcification.

MRI data were available for five patients. All scans showed markedly abnormal, atrophic/hypoplastic cerebral hemispheres with primitive sulcation. Progressive atrophy occurred in the one patient with serial scans. Cerebellar and/or brainstem atrophy was observed in three, and the corpus callosum was very small in all. Marked white matter volume loss and abnormal high T2 signal in cerebral white matter was common. Myelination was abnormal in all patients.

Calcification was apparent in all patients, most strikingly as a low-signal band on T2 but also as high signal on T1. Gyration was abnormal in all patients, with a very primitive gyral pattern, in some areas amounting to complete absence of gyration and a ribbon-like cortex. In other areas polymicrogyria was present. These changes were always symmetrical and had a frontoparietal predominance. Contrast enhancement did not occur in the two patients to whom it was given.

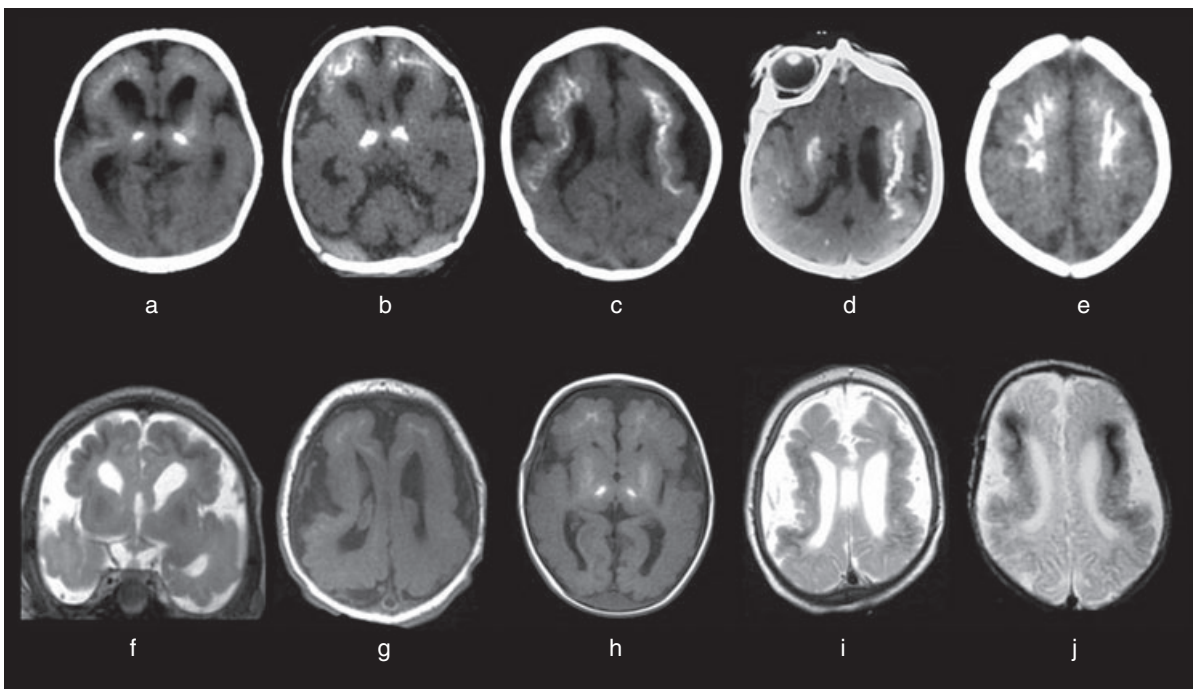

Figure 3: Band-like calcification with simplified gyration and polymicrogyria (BLC–PMG). Computed tomography (CT) scans showing typical features of BLC (a–e). Symmetrical thalamic calcification (a, b), largely symmetrical, fronto-parietal, predominantly deep cortical calcification (a–e), showing linear pattern (b,d,e) and reticular pattern (c). Magnetic resonance imaging (MRI) scans (f–j): coronal T2 (f), axial T1 (g, h), and axial T2 (i, j). Abnormal gyration with frontal or fronto-parietal predominance. There is a cortical malformation with polymicrogyria (g–j), and a ribbon-like cortex (i). Band-like cortical calcification visible as low signal on T2 (f, i j), and high signal T1 (g, h). Thalamic and basal ganglia calcification is apparent on T1 (h).

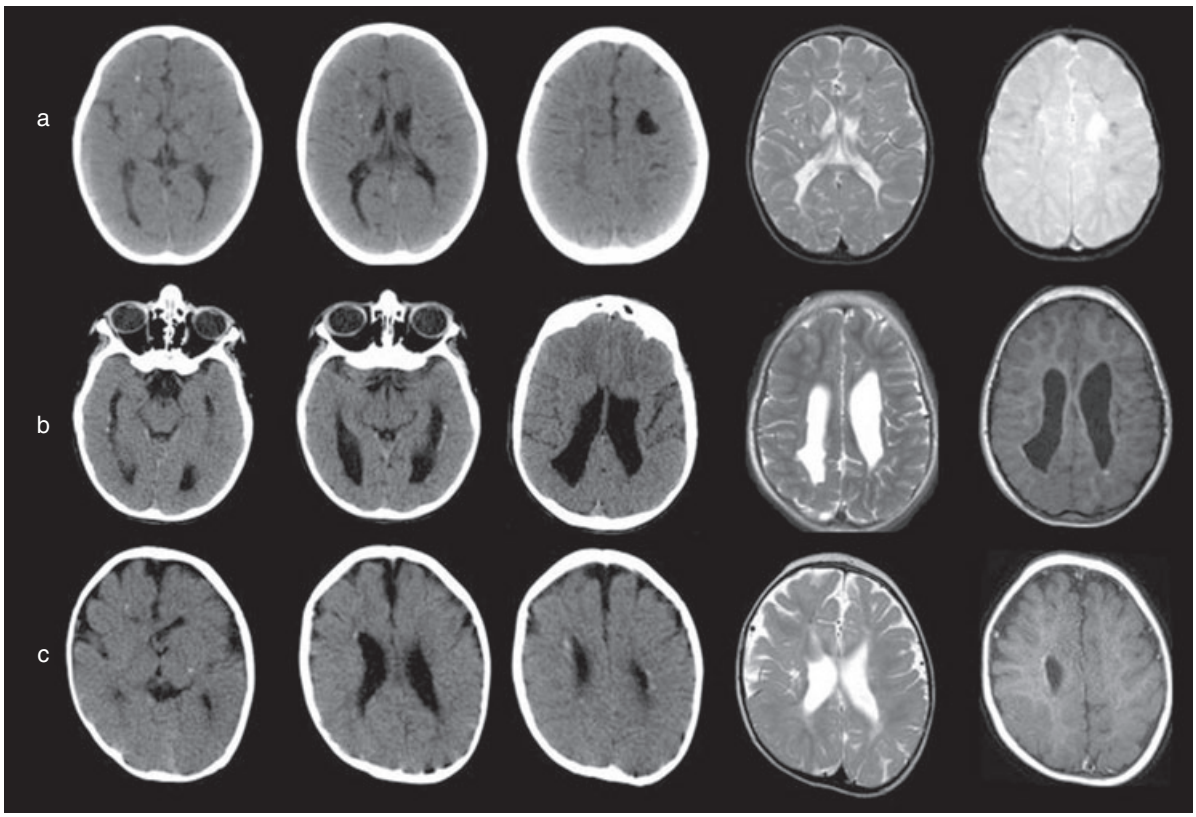

Figure 4: *COL4A1*-related disease in three patients. (Patient 1, row a; CT, axial T2 and axial gradient-echo MR, patients 2 and 3, rows b and c respectively; CT, axial T2 and axial T1 MR). CT in all patients demonstrates subtle spot or linear calcification in the periventricular region. Basal ganglia calcification (c) and deep white matter calcification (a,c) is present. Axial T2 and gradient-echo MR (a) and, axial T2 and T1 MR (b,c), demonstrate loss of periventricular white matter with angular ventricular outline and porencephaly (c), abnormal high signal in deep and periventricular white matter (a,c) and calcification visible as low signal spots on T2 sequences (a,c). Axial T1 images (b,c) demonstrate calcification as linear and spot high signal in the periventricular region and deep frontal white matter. Axial gradient-echo sequence (a) demonstrates a more diffuse `blush' of periventricular and deep white matter low signal. It is likely that this represents calcification, although micro-haemorrhage is a possibility.

COL4A1 mutation-related disease (Fig. 4)

CT data were available for three patients. The calcification was subtle but, taken together with the other radiological features, apparently characteristic. Periventricular spot and/or linear calcification was present in all patients. Spot calcification also occurred in the deep frontal and parietal white matter. Basal ganglia calcification was seen in two patients, and thalamic calcification in one.

MRI data were available for all patients. Calcification was observed in all patients, best seen as periventricular high signal on T1 sequences. Gradient echo sequences in one patient demonstrated calcification in the deep white matter. In all patients, features apparently characteristic of periventricular leukomalacia were present.[2,16] Specifically, these were angular dilatation of the lateral ventricles, loss of periventricular white matter with the cortical sulci almost reaching the margins of the lateral ventricle, and high signal on T2 or fluid-attenuated inversion-recovery sequences in the periventricular white matter. Porencephaly was present in one patient.

Other specific diagnoses (Fig. 5)

This group includes Degos[17,18] disease, infantile Krabbe disease,[19] juvenile Alexander disease,[20] chromosomal abnormality, and presumed mitochondrial disease. In these patients the diagnosis was made because of other clinical and radiological features, and the pattern of calcification was non-specific.

Cerebroretinal microangiopathy with calcification and cysts (Fig. 6)

CT data on 10 patients (15 scans) were available. Bilateral calcification was present in all patients but was asymmetrical in most. Where serial scans were available, progression in calcification was seen in three of six patients.

Cortical calcification was eventually present in all patients and was observed as early as 2 months of age. In contrast, two patients, one scanned at 2 and one at 3 months, did not yet show cortical calcification. Calcification was commonly seen in a frontoparietal distribution, but could involve all lobes or demonstrate an occipital predominance. In all patients, cortical calcification was predominantly in the depths of the sulci. In two

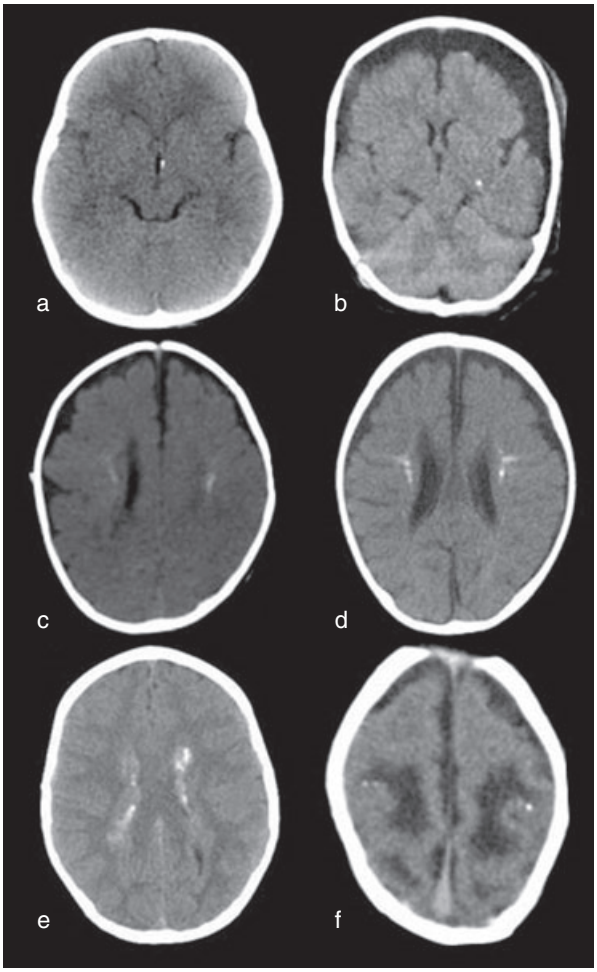

Figure 5: Other specific diagnoses. Degos disease demonstrating non-specific spot calcification (a, b). Infantile Krabbe disease (c, d), demonstrating symmetrical calcification within the corona radiata. Juvenile Alexander disease (e) demonstrating calcification within the abnormal periventricular garlands. Mitochondrial disease (f) showing deep cortical spot calcification with low-density white matter and simplified gyration.

patients, continuous gyral calcification was present. Spots of deep white matter calcification were present in six patients. In three early scans (at 2, 2, and 3mo), a diffuse blush of calcification was apparent in the cerebral white matter and basal ganglia (Fig. 6d). This disappeared on later scans. Basal ganglia calcification was present in all patients. Typically, this was seen as bilateral, but not always symmetrical, rock-like aggregates in the putamen, globus pallidus, caudate, and thalamus, and often in all of these sites. In three early scans, calcification was spot and blush. These patients went on to develop rock-like calcification on follow-up imaging (Fig. 6d,e).

Rock-like calcification in the cerebellum was common and could involve cortex, dentate nucleus, or white matter. Brainstem calcification was also seen. In some patients calcification in the wall of the cysts was observed. In the one patient in whom contrast was given, there was enhancement both in the basal ganglia and around the cysts.

MRI data were available for nine patients (13 scans). Of note, no scans showed cerebral or cerebellar atrophy. Ventricular dilatation was frequent. Abnormal white matter was present in all patients, seen as confluent high signal on T2 and fluid-attenuated inversion-recovery sequences. This could be markedly asymmetrical. The abnormal signal was periventricular and lobar in all patients, with U-fibre involvement in five patients, sometimes in a patchy distribution. All lobes could be involved. Some patients showed predominantly posterior involvement. Background myelination was normal in all patients. Three patients showed marked swelling and high signal of the pons and midbrain on T2-weighted imaging. Calcification was apparent in all patients, as both high and low signal on T2 and high signal on T1. Calcification involving the deep cortex along the white–grey junction was seen as a low signal serpiginous line on T2 images (Fig. 1i). Cysts were present in all patients, and contrast enhancement around the cysts and in the basal ganglia was seen in six out of seven patients to whom it was given. Cysts could occur in any location, but most commonly involved the brainstem, basal ganglia, or cerebral white matter. Posterior thalamic cysts enlarging into the lateral ventricles were also seen.

We specifically addressed the question whether a radiological distinction could be made between CRMCC-Coats-plus with *CTC1* mutations and CRMCC–LCC without *CTC1* mutations. We found no consistent differences.

Imaging characteristics in patients where the diagnosis is unknown

In 60 patients the aetiology of the observed ICC was unknown. This group showed a wide spectrum of clinical and radiological features. Within this cohort, some patients shared several similar features that enabled them to be subgrouped into putative categories (Table I).

Probable destructive mechanism

In eight patients the radiological features were suggestive of an acute or subacute destructive brain insult, such as hypoxia–ischaemia or haemorrhage (Fig. 7a,f). In two patients there was a relevant supporting history of such. In addition to ICC, the CT features included cortical and subcortical atrophy, multicystic encephalomalacia, and diffuse low attenuation involving white and grey matter. MRI features supporting this diagnosis were ulegyria, cortical highlighting, periventricular or cortical cystic changes, and signal change in the basal ganglia and thalami.

A further three patients had the features of periventricular leukomalacia and a pattern of periventricular calcification similar to the appearances seen in the patients described above with *COL4A1* mutation-related disease. Mutation testing of *COL4A1* was negative in two of these patients.

Calcification associated with polymicrogyria

CT images were available for six patients and MRI images for five patients (Fig. 7b,g). One patient had unilateral open

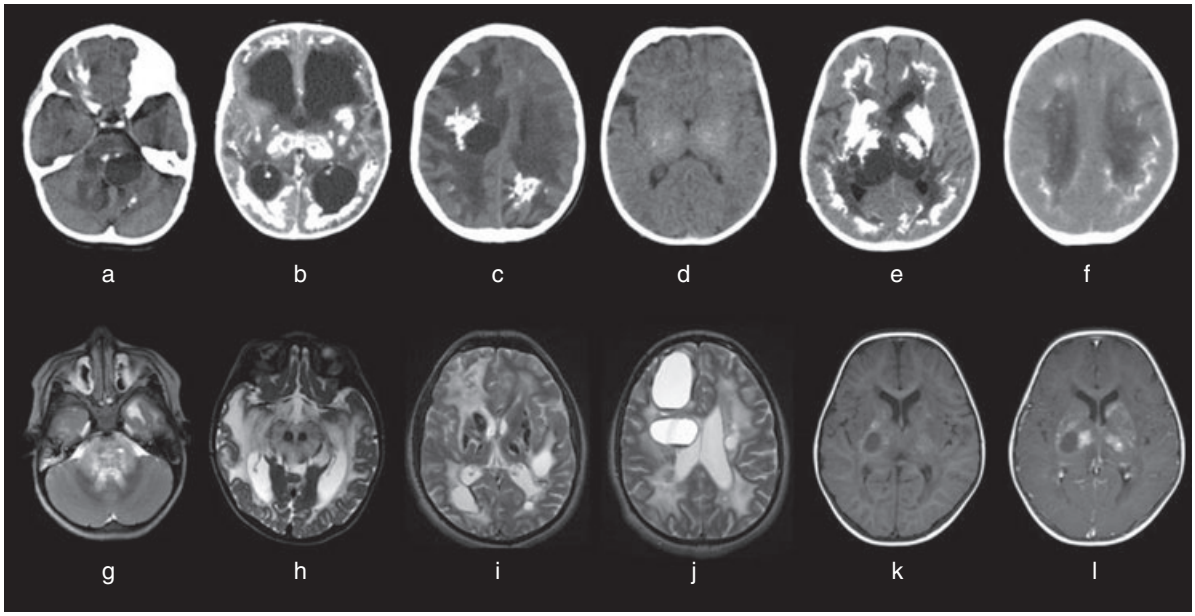

Figure 6: Cerebroretinal microangiopathy with calcification and cysts (CRMCC). Computed tomography (CT) (a–f), and magnetic resonance imaging (MR) (g–l). Typical CT appearances (a–c) showing calcification in cerebellum and pons and cyst in pons (a), dense calcification in thalami and basal ganglia, deep cortex and white-grey junction with hydrocephalus (b), and calcification around cyst in deep white matter and diffuse leukoencephalopathy (c). Serial CT scans at 2 months (d) and 4 years 6 months (e) showing dramatic progression from blush-like calcification of basal ganglia and frontal white matter (d) to the classical appearance (e). CT scan at 21 months (f), showing deep white matter spotty calcification and scalloped calcification in deep cortex and along white–grey junction. Axial T2 images demonstrating extensive high signal and swelling of brain stem (g, h), with probable calcification of the red nuclei (h). Typical T2 MR appearances (i, j), with diffuse, sometimes asymmetric white matter high signal, sparing U-fibres, cysts arising in deep white matter, and rock calcification in basal ganglia. Axial T1 MR, pre- (k) and post- (l) gadolinium showing contrast enhancement around calcified areas and a cyst within the basal ganglia.

lipped schizencephaly with polymicrogyria. Two non-identical twins had a pattern of frontoparietal polymicrogyria with cerebellar hypoplasia and thalamic calcification. Three patients had extensive polymicrogyria, hemispheric and often patchy white matter signal abnormalities and periventricular, basal ganglia, and cerebellar white matter calcification. In two patients there were cerebellar migrational abnormalities. The radiological phenotype was suggestive of congenital cytomegalovirus (CMV) infection in two of these patients even though investigations failed to confirm this.

Familial calcification with apparently characteristic involvement of the globus pallidus, posterior limb of the internal capsule, genu of the corpus callosum, and deep white matter

Three patients from the same family appeared to have a unique phenotype that we have so far recognized only in this single consanguineous pedigree from Qatar (Fig. 7c,h).[21] The pattern of calcification is apparently highly characteristic, involving the genu of the corpus callosum as well as the globus pallidus and deep white matter. The two affected children had neonatal seizures; one had developed normally whereas the other had mild to moderate learning difficulties. The affected mother had no cognitive or neurological abnormalities.

For the remaining 40 patients the cause of ICC remained unknown, and they could not be unequivocally assigned to any of the above groups. In some patients, the ICC appeared to be confined to the white (Fig. 7d,i), or grey matter (Fig. 7e,j). In others, the features were suggestive of congenital infection but this was not confirmed. In a further set of patients, AGS was considered but excluded on clinical and molecular grounds. At present, no common radiological pattern allows more precise grouping of these patients.

Dominant familial calcification was present in two families (seven patients), resembling what has been described as Fahr disease.

DISCUSSION

The value of a systematic approach to radiological phenotyping has been clearly demonstrated for white matter disorders[1,3,22] and brain malformation syndromes.[4–6] Here we present the results of a systematic study of radiological data from 119 patients demonstrating ICC on neuroimaging, and show that systematic phenotyping of ICC also allows recognizable patterns to be identified and, in some cases, disease entities to be characterized.

Importantly, early diagnosis can prevent unnecessary, expensive, and time-consuming investigations, thus sparing patients and their carers anxiety and distress.[3] Identifying

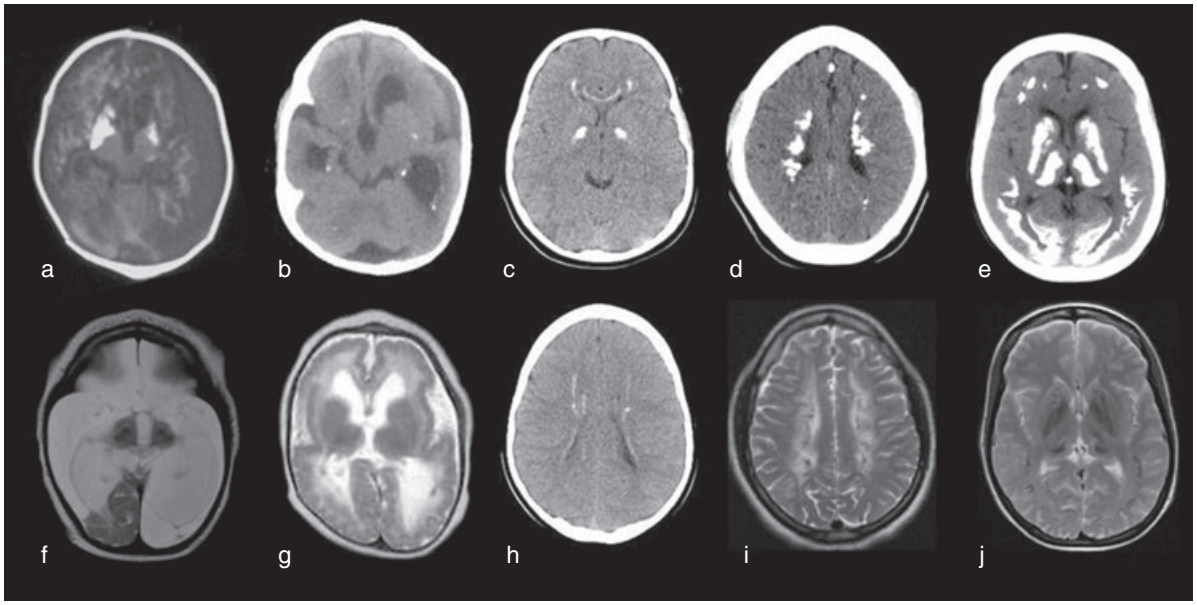

Figure 7: Examples of calcification where the aetiology is unknown. (a, f) Probable destructive mechanism. Computed tomography (CT) at 5 days of age (a) shows extensive destruction of both cerebral hemispheres, with high density within the abnormal cortex suggestive of haemorrhage or calcification. Dense calcification within both thalami is demonstrated. Axial T2 magnetic resonance (MR) images (f) at 16 months of age show liquefaction of both cerebral hemispheres with multicystic remnants. (b, g) Calcification with polymicrogyria (non-band-like calcification with simplified gyration and polymicrogyria type). CT (b) showing periventricular spot calcification, and axial T2 MR (g) showing fronto-parietal polymicrogyria and abnormal white matter. Appearances were suggestive of cytomegalovirus, but investigations did not confirm this. (c, h) Unique familial phenotype. Calcification in genu of corpus callosum, globus pallidus, and deep white matter in a male aged 8 years. An identical pattern was present in his sister and mother.[21] (d, i) Calcification predominantly within cerebral white matter. (e, j) Calcification predominantly within grey matter.

whether a disorder is genetic also allows appropriate counselling of parents and other relatives.

Pathological calcification occurs in response to many different processes, and thus probably represents the end-point of a diversity of insults. If calcification is the consequence of disordered calcium metabolism, it is usually described, confusingly, as metastatic. All other forms of pathological calcification are described as dystrophic, usually implying a previous or ongoing insult. There is a paucity of pathological data in children with ICC in general, and in the context of AGS,[23,24] CRMCC,[11] and BLC–PMG[10] in particular. The limited data that are available show that these genetically and clinically distinct disorders demonstrate calcification around blood vessels (BLC–PMG), and within the vessel wall (CRMCC and AGS). Pathological data from adults diagnosed with Fahr disease have also shown calcification in the vessel wall, alongside capillaries, and within the parenchyma.[25,26] Thus, the association of calcification with blood vessels may be a common feature of ICC, rather than revealing much about the underlying disease process.

Why calcification occurs in one location rather than another is unclear. There is undoubtedly a predilection for calcification of the basal ganglia. In this series, basal ganglia calcification was present in 116 (83%) of the 140 images, occurring in diverse disorders. Basal ganglia calcification alone is therefore of low specificity. These basic questions as to why calcification occurs, and why it is seen in particular locations in the brain, cannot be answered at present. This fact provides further justification for an approach to disease classification on the basis of radiological phenotyping. We propose that distinct phenotypes can be described for several disorders, and that there may be other phenotypes yet to be defined that will demonstrate radiological diagnostic specificity.

Aicardi–Goutieres syndrome

AGS is a Mendelian mimic of congenital infection,[27] which has been shown to be caused by mutations in any one of five genes encoding the DNA exonuclease TREX1,[28] the three non-allelic components of the RNase H2 endonuclease complex,[29] and the dNTP triphosphohydrolase SAMHD1.[30,31] There are patients with typical clinical and radiological features of AGS who do not have mutations in any of these genes, suggesting that there is at least one more gene associated with this phenotype. We have presented data on 33 patients with AGS, 27 of whom have mutations in one of the five known AGS-related genes. Although many different patterns of calcification may be seen in AGS (Fig. 2), there is a classical pattern that may be pathognomonic. Calcification may be seen on MRI, particularly as low-signal spots on T2 within the deep white matter, and the combination of calcification with a severe and characteristic white matter abnormality is diagnostic. In our series, calcification was apparent on MRI in only 15 out of 33 patients with AGS. This

emphasizes the importance of performing CT in the face of an unclassified white matter disorder. The MRI features of the severe neonatal or early infantile presentation are highly characteristic nonetheless. CT and MRI scans provide complementary data in AGS as for most of the phenotypes described in this study.

The most likely differential diagnosis to be considered in the context of AGS is that of congenital infection, congenital CMV in particular. However, the MRI features of congenital CMV are distinct and different.[32,33] Notably, in CMV, white matter abnormalities are usually patchy and often asymmetrical, with areas of normal myelination within the abnormal white matter. Polymicrogyria is common. Temporal cysts and temporal lobe swelling may occur in both disorders.

The autosomal recessive disorder cystic leukoencephalopathy without megalencephaly, caused by mutations in the *RNASET2* gene, results in a radiological phenotype virtually indistinguishable from congenital CMV,[34,35] and is thus generally distinct from the AGS radiological phenotype (although we note that relatively few mutation-positive cases have been published).

Although the classical pattern, described above, was common in our series, many other patterns of ICC can be seen in AGS, including very mild radiological phenotypes particularly associated with mutations in *RNASEH2B*. For this reason, we hold that AGS should be considered in any unexplained leukoencephalopathy.

Band-like calcification with simplified gyration and polymicrogyria

This is a rare disorder defined by its radiological phenotype, the recognition of which enabled the causative gene to be identified.[10] The radiological phenotype is best appreciated by considering both the CT and MRI appearances. In BLC–PMG a characteristic pattern of calcification occurs in a malformed brain. It is not only a cortical malformation, but a more global developmental/destructive abnormality. There is an abnormality of primary sulcation and the brain has a simplified 'hourglass' form. There is complete absence of gyri in some areas, but with a thin, rather sclerotic-looking, cortex quite different from that seen in type 1 or 2 lissencephaly. Both the brain malformation and the pattern of calcification are distinct from that seen in congenital CMV infection, which is the most common cause of the association of ICC with polymicrogyria. It is not yet known whether milder phenotypes occur, and if they might show radiological overlap with congenital infection.

COL4A1 mutation-related disease

Mutations in the *COL4A1* gene, encoding type IV collagen alpha 1, cause a genetic small-vessel disease affecting the brain, eyes, and kidneys.[36–39] *COL4A1* mutations lead to intracerebral haemorrhage and ischaemic damage that may have an ante-, peri-, or postnatal onset. Characteristically, but not exclusively, the disorder is associated with porencephaly.

In this series we identified three patients with *COL4A1* mutations and a characteristic radiological phenotype, associating periventricular leukomalacia and subtle periventricular, basal ganglia, and/or deep white matter calcification (Fig. 4). The diagnosis was considered because of the clinical features and suggestive imaging appearances. Periventricular leukomalacia is most commonly associated with preterm birth-related risk factors, and the presence of ICC is recognized in this context.[2] We have recently identified several cases demonstrating this pattern,[40] and we conclude that ICC may not be rare in *COL4A*-related disease. The combination of calcification with either porencephaly or irregular dilatation of lateral ventricles suggestive of periventricular leukomalacia should prompt consideration of *COL4A1* mutation testing when there is no history of preterm birth or other pre- or perinatal risk factors. The presence of eye abnormalities and/or a family history of cerebral palsy, aneurysm, stroke, eye disease (especially cataract), nephropathy, or muscle cramps are additional pointers to the diagnosis.

Cerebroretinal microangiopathy with calcification and cysts

At the time of the data analysis, it was not known whether all patients grouped under the umbrella term CRMCC had the same condition or discrete genetic disorders demonstrating the identical, or a very similar, radiological phenotype. From a clinical perspective, patients fall into two categories: those with a purely neurological disorder and those with significant extra-neurological involvement, notably retinopathy, bone, and gastrointestinal disease.[11,12] We have recently shown that mutations in *CTC1*, encoding conserved telomere maintenance component 1, cause Coats plus, a multisystem disorder the most characteristic features of which are retinal telangiectasia and exudates (Coats disease), ICC with an associated leukoencephalopathy and brain cysts, osteopenia with a tendency to fractures and poor bone healing, and a high risk of life-limiting gastrointestinal bleeding and portal hypertension caused by the development of vascular ectasias in the stomach, small intestine, and liver.[15] Mutations were not identified in any patient with a purely neurological disorder, indicating that LCC and Coats plus are distinct entities.

The patients described here all shared the three radiological features of ICC, leukoencephalopathy, and intraparenchymal cysts. This group of 10 comprised three patients with Coats plus who harboured *CTC1* mutations and seven with a purely neurological presentation. From a radiological perspective, there were no distinguishing features. The pattern of calcification is characteristic, but not on its own pathognomonic. White matter abnormalities are a hallmark of these disorders, and extensive confluent white-matter high signal on T2 images was seen in all patients. This could be markedly asymmetrical. Notably, background myelination was normal in all patients, and in many patients the peripheral white matter was spared or only patchily involved. Another feature of note was that cerebral atrophy did not occur in any patient.

Intracranial calcification cause undetermined

In 60 patients, half of our series, the cause of ICC remained undetermined. In 20 of these patients it was possible to sug-

gest a subgrouping based on shared radiological features. Notably, the clinical and radiological evidence suggested a possible destructive process in 11 patients. Attributing a destructive mechanism does not preclude a genetic cause, as illustrated by the three patients with *COL4A1* mutations.

The association of polymicrogyria and ICC is of particular interest. Although a growing number of genetic causes of PMG have been identified,[5,41–43] to our knowledge ICC has not been reported in any of these disorders.

In our series, two families (seven patients) demonstrated dominant inheritance of basal ganglia, with or without deep white-matter calcification. These are examples of what has loosely been called Fahr disease (synonyms striopallidodentate calcification, idiopathic basal ganglia calcification).[44] There is much confusion surrounding the use of Fahr disease as a diagnostic term. The published studies have used differing inclusion criteria, and often provide little detail of the radiological features. Even the more systematic studies have not provided detailed consideration of the radiological phenotype.[44] Fahr disease is almost certainly not a single entity, and may include different disorders resulting in a common and non-specific pattern of calcification. Familial and sporadic forms occur; some patients are asymptomatic, but in others a wide spectrum of clinical manifestations have been described, most commonly movement disorders, cognitive impairment, or psychiatric disease. Mutations in the *SLC20A2* gene, encoding the type III sodium-dependent phosphate transporter, have recently been identified in Fahr disease pedigrees from China, Brazil, and Spain.[45] It is likely that other discrete genetic subtypes will be identified.

CONCLUSION

We have shown that a systematic approach to describing the radiological phenotype of ICC allows consistent, recognizable patterns to be identified. These patterns may be specific for a given diagnosis, for example BLC–PMG, or strongly suggestive, for example AGS. Other patterns may indicate a mechanism such as a destructive cause. For many patients the aetiology remains obscure, but within this group some patterns can be identified that may represent distinct entities. We have shown that CT and MRI are complementary, and that for optimal diagnostic yield they should be considered together. We would recommend that CT be performed in all patients with an undefined neurological disorder in which MRI has not enabled a precise diagnosis. Gradient echo MRI will often demonstrate calcification, but is not as sensitive as CT, and the images produced have low definition and anatomical detail. Susceptibility-weighted MRI is highly sensitive to both blood and calcium and may prove of value in the future. For the moment, however, gradient-echo or susceptibility-weighted MRI should not be seen as a substitute for CT when the possibility of ICC is being considered. The potential for additional diagnostic information justifies the need for a further procedure.

Considering the premise of the present study, that is, to delineate the radiological characteristics of a set of scans showing ICC sent to the co-authors, our data set is inevitably characterized by a selection bias and non-blinded reporting. We are now exploring the use of an automated decision-tree analysis of imaging characteristics to produce a formalized descriptor set for ICC imaging analysis. Validation of this strategy will require the incorporation of data from a larger number of scans from patients with ICC of both known and unknown aetiology. We would hope that his methodology can then be tested in a blinded fashion for applicability by non-expert users. Such an approach may enable robust diagnostic categories to be determined.

ACKNOWLEDGEMENTS

We are very grateful to the families for their involvement in our research. YJC acknowledges the Manchester NIHR Biomedical Research Centre. This work received funding support from the Great Ormond Street Hospital Children's Charity and from the European Union's Seventh Framework Programme (FP7/2007-2013) under grant agreement number 241779, and from the Newlife Foundation for Disabled Children. We thank Dr Adeline Vanderver for her contribution to characterizing the radiological features of AGS. We also thank the following colleagues for referring patients: Salim Aftimos, Shay Ben Shachar, Natalie Boddaert, Luisa Bonafe, Alison Britland, Knut Brockmann, Paul Brogan, Kate Chandler, David Chitayat, Jill Clayton-Smith, Peter Corry, Christian de Goede, Maja Di Rocco, Dan Doherty, Ozdem Erturk, David Everman, Penny Fallon, Mahmood Fawzi, Bjorn Fischler, Caterina Garone, Simon Hammans, Michael Hutchinson, Anna Jansen, Sandeep Jayawant, Hulya Kayserili, Mary King, Rachel Kneen, Wilfrid Kratzer, Ram Kumar, Georg Kutschke, Ming Lim, Staffan Lundberg, Anirban Majumdar, Roger Massey, Allan McCarthy, Meriel McEntaggart, Ruth McGowan, Marianne McGuire, Ailsa McLellan, Ute Moog, Santosh Mordekar, Sakkubai Naidu, Luis Nunes, Anne O'Hara, Simona Orcesi, Katrin Ounap, Laura Panko, Alasdair Parker, Jayesh Patel, Mike Pike, Julie Prendiville, Katrina Prescot, Karen Pysden, Venkateswaran Ramesh, Tiina Remes, Cathlin Rice, Robert Robinson, Curtis Rogers, Gunter Scharer, Sunita Seal, Marco Seri, Concha Sierra Corcoles, Gayle Simpson, Calvin Soh, Helen Stewart, Kathryn Swodoba, Tiong Tan, Margaret Timmons, Graziela Uziel, Lionel Van Maldergem, Grace Vasallo, Emma Wakeling, Evangeline Wassmer, Andrea Whitney, Michel Willemsen, Nicole Wolf, Rhonda Wright, Jiang Yong-Hui, Andreas Zankl.

SUPPORTING INFORMATION

The following additional material may be found online.

Table SI: (a) Summary of categories scored in the computed tomography database. (b) Summary of categories scored in the magnetic resonance imaging database.

Table S2: Characteristics of calcification.

REFERENCES

1. van der Knaap MS, Breiter SN, Naidu S, Hart AAM, Valk J. Defining and categorizing leukoencephalopathies of unknown origin: MR imaging approach. *Radiology* 1999; **213:** 121–33.
2. van der Knaap MS, Valk J. Magnetic Resonance of Myelination and Myelin Disorders. 3rd edn. Berlin: Springer, 2005.

3. Schiffmann R, van der Knaap MS. Invited article: an MRI-based approach to the diagnosis of white matter disorders. *Neurology* 2009; **72:** 750–9.
4. Barkovich AJ, Kuzniecky RI, Jackson GD, Guerrini R, Dobyns WB. A developmental and genetic classification for malformations of cortical development. *Neurology* 2005; **65:** 1873–87.
5. Bahi-Buisson N, Poirier K, Boddaert N, et al. GPR56-related bilateral frontoparietal polymicrogyria: further evidence for an overlap with the cobblestone complex. *Brain* 2010; **133:** 3194–209.
6. Namavar Y, Barth PG, Kasher PR, et al. Clinical, neuroradiological and genetic findings in pontocerebellar hypoplasia. *Brain* 2011; **134:** 143–56.
7. Abdel-Salem GM, Zaki MS, Saleem SN, Gaber KR. Microcephaly, malformation of brain development and intracranial calcification in sibs: pseudo-TORCH or a new syndrome. *Am J Med Genet A* 2008; **146:** 2929–36.
8. Briggs TA, Wolf NI, D'Arrigo S, et al. Band-like intracranial calcification with simplified gyration and polymicrogyria: a distinct "pseudo-TORCH" phenotype. *Am J Med Genet A* 2008; **146:** 3173–80.
9. Abdel-Salam GM, Zaki MS. Band-like intracranial calcification (BIC), microcephaly and malformation of brain development: a distinctive form of congenital infection like syndrome. *Am J Med Genet A* 2009; **149:** 1565–8.
10. O'Driscoll MC, Daly SB, Urquhart JE, et al. Recessive mutations in the gene encoding the tight junction protein occludin cause band-like calcification with simplified gyration and polymicrogyria. *Am J Hum Genet* 2010; **87:** 354–64.
11. Linnankivi T, Valanne L, Paetau A, et al. Cerebroretinal microangiopathy with calcifications and cysts. *Neurology* 2006; **67:** 1437–43.
12. Briggs TA, Abdel-Salam GMH, Balicki M, et al. Cerebroretinal microangiopathy with calcifications and cysts (CRMCC). *Am J Med Genet A* 2008; **146:** 182–90.
13. Crow YJ, McMenamin J, Haengelli CA, et al. Coats' plus: a progressive familial syndrome of bilateral Coats' disease, characteristic cerebral calcification, leukoencephalopathy, slow pre- and post-natal linear growth and defects of bone marrow and integuement. *Neuropediatrics* 2004; **35:** 10–9.
14. Labrune P, Lacroix C, Goutières F, et al. Extensive brain calcifications, leukodystrophy, and formation of parenchymal cysts: a new progressive disorder due to diffuse cerebral microangiopathy. *Neurology* 1996; **46:** 1297–301.
15. Anderson BH, Kasher PR, Mayer J, et al. Mutations in *CTC1*, encoding conserved telomere maintenance component 1, cause Coats plus. *Nat Genet* 2012; **44:** 338–42.
16. Barkovich AJ. Pediatric Neuroimaging. 4th edn. Philadelphia: Lippincott Williams & Wilkins, 2005.
17. Moss C, Wassmer E, Debelle G, et al. Degos disease: a new simulator of non-accidental injury. *Dev Med Child Neurol* 2009; **51:** 647–50.
18. Yeo TH, Vassallo G, Judge M, Laycock N, Kelsey A, Crow YJ. Infantile neurological Degos disease. *Eur J Pediatr Neurol* 2011; **15:** 167–70.
19. Livingston JH, Graziano C, Pysden K, et al. Intracranial calcification in early infantile Krabbe disease: nothing new under the sun. *Dev Med Child Neurol* 2011; **54:** 376–9.
20. Jefferson RJ, Absoud M, Jain R, et al. Alexander disease with periventricular calcification: a novel mutation of the GFAP gene. *Dev Med Child Neurol* 2010; **52:** 1160–3.
21. Elsaid MF, Crow YJ, Livingston JH, Ben-Omran T. New subtype of familial intracranial calcification in a mother and two children. *Am J Med Genet A* 2010; **152:** 943–6.
22. van der Knaap MS, Valk J, de Neeling N, Nauta JJP. Pattern recognition in magnetic resonance imaging of white matter disorders in children and young adults. *Neuroradiology* 1991; **33:** 478–93.
23. Barth PG, Walter A, van Gelderen I. Aicardi–Goutières syndrome: a genetic microangiopathy? *Acta Neuropathol* 1999; **98:** 212–6.
24. Barth PG. The neuropathology of Aicardi–Goutières syndrome. *Eur J Pediatr Neurol* 2002; **6:**(Suppl. A) 26–31.
25. Duckett S, Galle P, Escourolle R, Poirier J, Hauw JJ. Presence of zinc, aluminum, magnesium in striopallidodentate (SPD) calcifications (Fahr's disease): electron probe study. *Acta Neuropathol (Berl)* 1977; **38:** 7–10.
26. Fujita D, Terada S, Ishizu H, et al. Immunohistochemical examination on intracranial calcification in neurodegenerative diseases. *Acta Neuropathol* 2003; **105:** 259–64.
27. Crow YJ, Livingston JH. Aicardi–Goutieres syndrome: an important Mendelian mimic of congenital infection. *Dev Med Child Neurol* 2008; **50:** 410–6.
28. Crow YJ, Hayward BE, Parmar R, et al. Mutations in the gene encoding the 3′–5′ DNA exonuclease TREX1 cause Aicardi–Goutières syndrome at the *AGS1* locus. *Nat Genet* 2006; **38:** 917–20.
29. Crow YJ, Leitch A, Hayward BE, et al. Mutations in genes encoding ribonuclease H2 subunits cause Aicardi–Goutières syndrome and mimic congenital viral brain infection. *Nat Genet* 2006; **38:** 910–6.
30. Rice GI, Bond J, Asipu A, et al. Mutations involved in Aicardi–Goutières syndrome implicate *SAMHD1* as regulator of the innate immune response. *Nat Genet* 2009; **41:** 829–32.
31. Goldstone DC, Ennis-Adeniran V, Hedden JJ, et al. HIV-1 restriction factor SAMHD1 is a deoxynucleoside triphosphate triphosphohydrolase. *Nature* 2011; **480:** 379–82.
32. de Vries LS, Gunardi H, Barth PG, Bok LA, Verboon-Maciolek MA, Groenendaal F. The spectrum of cranial ultrasound and magnetic resonance imaging abnormalities in congenital cytomegalovirus infection. *Neuropediatrics* 2004; **35:** 113–9.
33. van der Knaap MS, Vermeulen G, Barkhof F, Hart AAM, Loeber JG, Weel JFL. Pattern of white matter abnormalities at MR imaging: use of polymerase chain reaction testing of guthrie cards to link pattern with congenital cytomegalovirus infection. *Radiology* 2004; **230:** 529–36.
34. Henneke M, Preuss N, Engelbrecht V, et al. Cystic leukoencephalopathy without megalencephaly: a distinct disease entity in 15 children. *Neurology* 2005; **64:** 1411–6.
35. Henneke M, Diekmann S, Ohlenbusch A, et al. RNASET2-deficient cystic leukoencephalopathy resembles congenital cytomegalovirus brain infection. *Nat Genet* 2009; **41:** 773–5.
36. Vahedi K, Massin P, Guichard JP, et al. Hereditary infantile hemiparesis, retinal arteriolar tortuosity, and leukoencephalopathy. *Neurology* 2003; **60:** 57–63.
37. Breedveld G, de Coo IF, Lequin MH, et al. Novel mutations in three families confirm a major role of COL4A1 in hereditary porencephaly. *J Med Genet* 2006; **43:** 490–5.
38. Vahedi K, Kubis N, Boukobza M, et al. COL4A1 mutation in a patient with sporadic, recurrent intracerebral hemorrhage. *Stroke* 2007; **38:** 1461–4.
39. Mine M, Tournier-Lasserve E. Intracerebral haemorrhage and *COL4A1* mutations, from preterm infants to adult patients. *Ann Neurol* 2009; **65:** 1–2.
40. Livingston JH, Doherty D, Orcesi S, et al. *COL4A1* mutations associated with a characteristic pattern of intracranial calcification. *Neuropediatrics* 2011; **42:** 227–33.
41. Abdollahi MR, Morrison E, Sirey T, et al. Mutation of the variant alpha tubulin TUBA8 results in polymicrogyria with optic nerve hypoplasia. *Am J Hum Genet* 2009; **85:** 737–44.
42. Jaglin XH, Poirier K, Saillour Y, et al. Mutations in the beta-tubulin gene *TUBB2B* result in asymmetrical polymicrogyria. *Nat Genet* 2009; **41:** 746–52.
43. Hehr U, Schuierer G. Genetic assessment of cortical malformations. *Neuropediatrics* 2011; **42:** 43–50.
44. Manyam BV. What is and what is not "Fahr's disease"? *Parkinsonism Relat Disord* 2005; **11:** 73–80.
45. Wang C, Li Y, Shi L, et al. Mutations in SLC20A2 link familial idiopathic basal ganglia calcification with phosphate homeostasis. *Nat Genet* 2012; **44:** 254–6.